

IEEE TRANSACTIONS ON INDUSTRY APPLICATIONS

A PUBLICATION OF THE IEEE INDUSTRY APPLICATIONS SOCIETY

WWW.IEEE.ORG/IAS



SERVING OUR MEMBERS AND SUBSCRIBERS IN OUR FORTY-EIGHTH YEAR OF PUBLICATION

NOVEMBER/DECEMBER 2012

VOLUME 48

NUMBER 6

ITIACR

(ISSN 0093-9994)

JOINTLY PREPARED WITH THE IEEE TRANSACTIONS ON POWER ELECTRONICS
(With Special Distribution to IEEE Transactions on Power Electronics Subscribers)

SPECIAL ISSUE ON ELECTRIC MACHINES AND DRIVES IN EMERGING APPLICATIONS, 2012

Introduction to the Special Issue on Electric Machines and Drives in Emerging Applications, 2012	<i>Olorunfemi Ojo and F. Dong Tan</i>	1776
<hr/>		
<i>Testing and Design of Permanent-Magnet Generators</i>		
Regenerative Testing of a Concentrated-Winding Permanent-Magnet Synchronous Machine for Offshore Wind Generation—Part I: Test Concept and Analysis	<i>Fabio Luise, Stefano Pieri, Mario Mezzarobba, and Alberto Tassarolo</i>	1779
Regenerative Testing of a Concentrated-Winding Permanent-Magnet Synchronous Machine for Offshore Wind Generation—Part II: Test Implementation and Results	<i>Fabio Luise, Stefano Pieri, Mario Mezzarobba, and Alberto Tassarolo</i>	1791
Magnetic System Study of a Compound-Structure Permanent-Magnet Synchronous Machine for HEVs	<i>Yong Liu, Dansong Cheng, Yi Sui, Jingang Bai, Chengde Tong, and Weiming Tong</i>	1797
Design of a Flux-Switching Electrical Generator for Wind Turbine Systems	<i>Javier Ojeda, Marcelo Godoy Simões, Guangjin Li, and Mohamed Gabsi</i>	1808
Experimental Evaluation and Predictive Control of an Air-Cored Linear Generator for Direct-Drive Wave Energy Converters	<i>Rieghard Vermaak and Maarten J. Kamper</i>	1817
Design of a Sustainable Wind Generator System Using Redundant Materials	<i>Hartmut Jagau, M. Azeem Khan, and Paul S. Barendse</i>	1827
<i>Fault Detection and Tolerance in Motor Drives</i>		
Static Eccentricity Fault Detection in Single-Stator–Single-Rotor Axial-Flux Permanent-Magnet Machines	<i>Seyyed Mehdi Mirimani, Abolfazl Vahedi, Fabrizio Marignetti, and Enzo De Santis</i>	1838

(Contents Continued on Page 1773)



Single-Turn Fault Detection in Induction Machine Using Complex-Wavelet-Based Method	1846
. <i>Jeevanand Seshadrinath, Bhim Singh, and Bijaya K. Panigrahi</i>	
Fault-Tolerant Operation of a Fully Electric Gearbox Equivalent	1855
. <i>Thomas Gerrits, Cornelis G. E. Wijnands, Johannes J. H. Paulides, and Jorge L. Duarte</i>	
Condition Monitoring of DC-Link Capacitors in Aerospace Drives	1866
. <i>Andrew Wechsler, Barrie C. Mecrow, David J. Atkinson, John W. Bennett, and Mamar Benarous</i>	
<i>Loss and Efficiency Determination in Electric Machines</i>	
High-Efficiency Current Excitation Strategy for Variable-Speed Nonsinusoidal Back-EMF PMSM Machines	1875
. <i>Parag Kshirsagar and R. Krishnan</i>	
An Algorithm for Nonintrusive <i>In Situ</i> Efficiency Estimation of Induction Machines Operating With Unbalanced Supply Conditions	1890
. <i>Arbi Gharakhani Siraki, Chetan Gajjar, Mohamed Azeem Khan, Paul Barendse, and Pragasen Pillay</i>	
Analysis of Iron and Magnet Losses in Surface-Permanent-Magnet Machines Resulting From Injection-Based Self-Sensing Position Estimation	1901
. <i>Shih-Chin Yang and Robert D. Lorenz</i>	
Comparison of Two Methods for Full-Load <i>In Situ</i> Induction Motor Efficiency Estimation From Field Testing in the Presence of Over/Undervoltages and Unbalanced Supplies	1911
. <i>Arbi Gharakhani Siraki and Pragasen Pillay</i>	
<i>Sensorless and Advanced Motor Control</i>	
Encoderless Servo Drive With Adequately Designed IPMSM for Pulse-Voltage-Injection-Based Position Detection	1922
. <i>Sohji Murakami, Takayuki Shiota, Motomichi Ohto, Kozo Ide, and Masaki Hisatsune</i>	
High-Frequency-Injection-Assisted “Active-Flux”-Based Sensorless Vector Control of Reluctance Synchronous Motors, With Experiments From Zero Speed	1931
. <i>Sorin-Cristian Agarlita, Ion Boldea, and Frede Blaabjerg</i>	
A Hysteresis Hybrid Extended Kalman Filter as an Observer for Sensorless Valve Control in Camless Internal Combustion Engines.	1940
. <i>Paolo Mercorelli</i>	
Motion-Sensorless Control of BLDC-PM Motor With Offline FEM-Information-Assisted Position and Speed Observer	1950
. <i>Alin Ştirban, Ion Boldea, and Gheorghe-Daniel Andreescu</i>	
Comparison of a Reduced-Order Observer and a Full-Order Observer for Sensorless Synchronous Motor Drives	1959
. <i>Toni Tuovinen, Marko Hinkkanen, Lennart Harnefors, and Jorma Luomi</i>	
Sensorless Vector Control of PM Synchronous Motors During Single-Phase Open-Circuit Faulted Conditions	1968
. <i>Alberto Gaeta, Giacomo Scelba, and Alfio Consoli</i>	
High-Bandwidth Explicit Model Predictive Control of Electrical Drives.	1980
. <i>Sébastien Mariéthoz, Alexander Domahidi, and Manfred Morari</i>	
Control of a Synchronous Motor With an Inverter Integrated Rotor	1993
. <i>Eunsoo Jung, Sungmin Kim, Jung-Ik Ha, and Seung-Ki Sul</i>	
<i>Multiphase Motor Drives and Converters</i>	
Effect of Current Harmonic Injection on Constant Rotor Volume Multiphase Induction Machine Stators: A Comparative Study	2002
. <i>Ayman S. Abdel-Khalik, Mahmoud I. Masoud, Shehab Ahmed, and Ahmed M. Massoud</i>	
Multiphase Cage-Rotor Induction-Machine Drive With Direct Implementation of Brush DC Operation.	2014
. <i>Nkosinathi Gule and Maarten J. Kamper</i>	
A Novel Control Strategy Applicable for a Dual AC Drive With Common Mechanical Load	2022
. <i>Ioannis X. Bogiatzidis, Athanasios N. Safacas, Epaminondas D. Mitronikas, and George A. Christopoulos</i>	
A Hybrid Five-Level Inverter With Common-Mode Voltage Elimination Having Single Voltage Source for IM Drive Applications	2037
. <i>P. P. Rajeevan and K. Gopakumar</i>	
Position Control of a Multi-Motor Drive Based on Series-Connected Five-Phase Tubular PM Actuators	2048
. <i>Michele Mengoni, Angelo Tani, Luca Zarri, Giovanni Serra, and Domenico Casadei</i>	
Reduction of Common-Mode Voltage in Five-Phase Induction Motor Drives Using Predictive Control Techniques	2059
. <i>Mario J. Durán, Jose A. Riveros, Federico Barrero, Hugo Guzmán, and Joel Prieto</i>	
Sensorless Rotor Position Detection Capability of a Dual Three-Phase Fractional-Slot IPM Machine	2068
. <i>Massimo Barcaro, Adriano Faggion, Nicola Bianchi, and Silverio Bolognani</i>	
On the Common-Mode Voltage in Multilevel Multiphase Single- and Double-Ended Diode-Clamped Voltage-Source Inverter Systems	2079
. <i>Sosthenes Karugaba, Annette Muetze, and Olorunfemi Ojo</i>	
Analysis of Fault-Tolerant Multiphase Power Converter for a Nine-Phase Permanent Magnet Synchronous Machine	2092
. <i>Mircea Ruba and Daniel Fodorean</i>	
A Carrier-Based PWM Modulation Technique for Balanced and Unbalanced Reference Voltages in Multiphase Voltage-Source Inverters.	2102
. <i>Sosthenes Karugaba and Olorunfemi Ojo</i>	

A Dual Five-Phase Space-Vector Modulation Algorithm Based on the Decomposition Method	2110
. <i>Martin Jones, I. Nyoman Wahyu Satiawan, Nandor Bodo, and Emil Levi</i>	
<i>Design of Converters for Motor Drives</i>	
Power-Dense Shipboard-Compatible Low-Horsepower Variable-Frequency Drives	2121
. <i>Robert Cuzner, Daniel Drews, William Kranz, Ashish Bendre, and Giri Venkataramanan</i>	
Multiport Converter for Fast Charging of Electrical Vehicle Battery	2129
. <i>Gierry Waltrich, Jorge L. Duarte, and Marcel A. M. Hendrix</i>	
Low-Voltage AC Drive Based on Double-Sided Cooled IGBT Press-Pack Modules	2140
. <i>Slavo Kicin, Matti Laitinen, Christoph Haederli, Jukka Sikanen, Roman Grinberg, Chunlei Liu, J.-H. Fabian, and Amina Hamidi</i>	
Design of Drives for Inverter-Assisted Induction Generators	2147
. <i>Max Myers, Marc Bodson, and Faisal Khan</i>	
<i>Design of Machines for Drive Applications</i>	
Concurrent Design of Interior-Permanent-Magnet Machines for Self-Sensing and Power Conversion	2157
. <i>Natee Limsuwan, Takashi Kato, and Robert D. Lorenz</i>	
Spatial Discretization Methods for Air Gap Permeance Calculations in Double Salient Traction Motors	2165
. <i>Esin Ilhan, Maarten F. J. Kremers, Emilia T. Motoasca, Johan J. H. Paulides, and Elena A. Lomonova</i>	
Estimation of Airgap Length in Magnetically Levitated Systems	2173
. <i>Amir H. Ranjbar, Ricardo Noboa, and Babak Fahimi</i>	
Comparison of Calculation Methods for Hybrid Stepping Motors	2182
. <i>Cornelia Stuebig and Bernd Ponick</i>	
Recent Advances in Axial-Flux Permanent-Magnet Machine Technology	2190
. <i>Fabio Giulii Capponi, Giulio De Donato, and Federico Caricchi</i>	
Investigation of Exterior Rotor Bearingless Motor Topologies for High-Quality Mixing Applications	2206
. <i>Thomas Reichert, Thomas Nussbaumer, and Johann W. Kolar</i>	
Topology Comparison of Compound-Structure Permanent-Magnet Synchronous Machines.	2217
. <i>Yong Liu, Dansong Cheng, Jingang Bai, Chengde Tong, Zhiyi Song, and Weiming Tong</i>	
Segmental Stator Switched Reluctance Machine for Safety-Critical Applications.	2223
. <i>Loránd Szabó and Mircea Ruba</i>	
Electromagnetic Design and Control Strategy of an Axially Magnetized Permanent-Magnet Linear Alternator for Free-Piston Stirling Engines.	2230
. <i>Ping Zheng, Chengde Tong, Jingang Bai, Bin Yu, Yi Sui, and Wei Shi</i>	
Coupled Electromagnetic-Thermal-Mechanical Analysis for Accurate Prediction of Dual-Mechanical-Port Machine Performance	2240
. <i>Xikai Sun, Ming Cheng, Sa Zhu, and Jianzhong Zhang</i>	
Novel Modular-Rotor Switched-Flux Permanent Magnet Machines	2249
. <i>A. S. Thomas, Z. Q. Zhu, and L. J. Wu</i>	
Permanent-Magnet Flux-Switching Synchronous Motor Employing a Segmental Rotor	2259
. <i>Ackim Zulu, Barrie C. Mecrow, and Matthew Armstrong</i>	
Optimized Design of PM Torquer for Dynamically Tuned Gyroscope.	2268
. <i>Mohammadhossein Barzegari Bafghi, Abolfazl Vahedi, and Javad Soleimani</i>	
Optimization of the Winding Arrangement to Increase the Zero-Sequence Inductance of a Synchronous Machine With Multifunctional Converter Drive	2277
. <i>Thomas Hackner, Johannes Pfforr, Henk Polinder, and Jan Abraham Ferreira</i>	
A High-Torque-Density Permanent-Magnet Free Motor for in-Wheel Electric Vehicle Application.	2287
. <i>Saurabh P. Nikam, Vandana Rallabandi, and B. G. Fernandes</i>	
<i>Comparative Analysis of Motor Drives</i>	
Multilayer-Winding Versus Switched-Flux Permanent-Magnet AC Machines for Gearless Applications in Clean-Energy Systems	2296
. <i>Oleksandr Dobzhanskyi, Pavani Gottipati, Ekrem Karaman, Xiaozhong Luo, Ernest A. Mendrela, and Andrzej M. Trzynadlowski</i>	
Design of Switched Reluctance Motor Competitive to 60-kW IPMSM in Third-Generation Hybrid Electric Vehicle	2303
. <i>Kyohei Kiyota and Akira Chiba</i>	
Direct Comparison of Induction Motor and Line-Start IPM Synchronous Motor Characteristics for Semi-Hermetic Compressor Drives.	2310
. <i>Bojan Štumberger, Tine Marčič, and Miralem Hadžiselimović</i>	
Comparison of Induction and PM Synchronous Motor Drives for EV Application Including Design Examples	2322
. <i>Gianmario Pellegrino, Alfredo Vagati, Barbara Boazzo, and Paolo Guglielmi</i>	
Consideration of Number of Series Turns in Switched-Reluctance Traction Motor Competitive to HEV IPMSM	2333
. <i>Akira Chiba, Motoki Takeno, Nobukazu Hoshi, Masatsugu Takemoto, Satoshi Ogasawara, and M. Azizur Rahman</i>	
Comparison of Induction Motor and Line-Start IPM Synchronous Motor Performance in a Variable-Speed Drive	2341
. <i>Tine Marčič, Bojan Štumberger, and Gorazd Štumberger</i>	

Control of Motor Drives and Generators

Magnet Temperature Estimation in Surface PM Machines During Six-Step Operation	2353
. <i>David Díaz Reigosa, Fernando Briz, Michael W. Degner, Pablo García, and Juan M. Guerrero</i>	
Robust Passivity-Based Control of a Buck–Boost-Converter/DC-Motor System: An Active Disturbance Rejection Approach	2362
. <i>Jesús Linares-Flores, Jorge L. Barahona-Avalos, Hebertt Sira-Ramírez, and Marco A. Contreras-Ordaz</i>	
Sliding-Mode Control of Wave Power Generation Plants	2372
. <i>Aitor J. Garrido, Izaskun Garrido, Modesto Amundarain, Mikel Alberdi, and Manuel De la Sen</i>	
Comparative Study of PMSM Drive Systems Based on Current Control and Direct Torque Control in Flux-Weakening Control Region	2382
. <i>Yukinori Inoue, Shigeo Morimoto, and Masayuki Sanada</i>	
Novel Field-Weakening Control Scheme for Permanent-Magnet Synchronous Machines Based on Voltage Angle Control	2390
. <i>David Stojan, Dušan Drevenšek, Željko Plantič, Bojan Grčar, and Gorazd Štumberger</i>	
Implementation and Sensorless Vector-Control Design and Tuning Strategy for SMPM Machines in Fan-Type Applications	2402
. <i>Parag Kshirsagar, Rolando P. Burgos, Jihoon Jang, Alessandro Lidozzi, Fei Wang, Dushan Boroyevich, and Seung-Ki Sul</i>	
Stand-Alone Single-Phase Power Generation Employing a Three-Phase Isolated Asynchronous Generator	2414
. <i>Bhim Singh and Shailendra Sharma</i>	
Active Torque Control for Gearbox Load Reduction in a Variable-Speed Wind Turbine	2424
. <i>Goran Mandic, Adel Nasiri, Eduard Muljadi, and Francisco Oyague</i>	
Modified Indirect Vector Control Technique for Current-Source Induction Motor Drive	2433
. <i>Ahmed K. Abdelsalam, Mahmoud I. Masoud, Mostafa S. Hamad, and Barry W. Williams</i>	

This issue of IEEE TRANSACTIONS ON INDUSTRY APPLICATIONS is available on the World Wide Web. Access will be limited to members of the IEEE Industry Applications Society and other subscribers. Members may subscribe to the traditional printed copy of each issue. Contact Member Services Department: +1800 678 IEEE; FAX: +1732 562 6380; e-mail: member-services@ieee.org; for subscription rates and information.

To access IEEE TRANSACTIONS ON INDUSTRY APPLICATIONS, log into the IEEE Home Page, <http://www.ieee.org>, and click on *IEEE Xplore*. If this is your first visit to this site, you must establish an IEEE Web account. Click on “Establish IEEE Web Account” and follow the instructions. You will choose a user name and password to use for future logins, and be given access to those IEEE publications to which you are entitled. To reach IAS publications, click on “Journals and Magazines” and type Industry Applications in the search field. IAS members may access all issues dated 1988 and later. To read, download, or print full papers, you will need Adobe Acrobat Reader, which can be downloaded free if you do not already have it.

For general information about the IEEE Industry Applications Society, refer to the IAS Home Page at <http://www.ieee.org/ias/>.



IEEE INDUSTRY APPLICATIONS SOCIETY

The scope of the Industry Applications Society, as a transnational organization, is the advancement of the theory and practice of electrical and electronic engineering in the development, design, manufacture, and application of electrical systems, apparatus, devices, and controls to the processes and equipment of industry and commerce; the promotion of safe, reliable, and economic installations; industry leadership in energy conservation and environmental, health, and safety issues; the creation of voluntary engineering standards and recommended practices; and the professional development of its membership. Papers within the scope of the society can be submitted for publication in the TRANSACTIONS. All members of the IEEE are eligible for membership in the Society and will receive free access to the online version of this TRANSACTIONS as part of their annual Society membership fee of \$20. The print version of the TRANSACTIONS is also available to IEEE IAS members for an additional \$25, and to other IEEE members for \$50 per year. Special rates for students, retirees, etc., may apply. For information on joining or subscribing, write to the IEEE at the address below. *Member copies of Transactions/Journals are for personal use only.*

SOCIETY EXECUTIVE BOARD Society Officers and Past President

<i>President</i> BRUNO LEQUESNE Eaton Corporation Milwaukee, WI bruno.lequesne@ieee.org	<i>President-Elect</i> BLAKE LLOYD Iris Power Mississauga, ON, Canada BlakeLloyd@ieee.org	<i>Vice President</i> DAVID DUROCHER Eaton Electrical Wilsonville, OR daviddurocher@eaton.com	<i>Treasurer</i> DONALD S. ZINGER Northern Illinois University DeKalb, IL d.zinger@ieee.org	<i>Past President</i> THOMAS A. NONDAHL Rockwell Automation Milwaukee, WI t.nondahl@ieee.org
---	---	---	---	--

Technical Department Chairs

<i>Industrial and Commercial Power Systems</i> T. DAVID MILLS d.mills@ieee.org	<i>Industrial Power Conversion Systems</i> JOSEPH OJO jojo@tntech.edu	<i>Manufacturing Systems Development and Applications</i> GEORGES ZISSIS georges.zissis@laplace.univ-tlse.fr	<i>Process Industries</i> RODERICK H. SIMMONS roderick.simmons@buzziunicemusa.com
--	---	--	---

Operating Department Chairs

<i>Awards</i> ANDREW BAGLEY atbagley@ra.rockwell.com	<i>Chapters and Membership</i> PETER MAGYAR peter.magyar@ieee.org	<i>Education</i> JOSEPH SOTTILE jsottile@enr.uky.edu	<i>Meetings</i> R. MARK NELMS m.nelms@ieee.org	<i>Publications</i> AHMED RUBAAI arubai@Howard.edu	<i>Standards</i> S. MARK HALPIN halpin@eng.auburn.edu
<i>Constitution and Bylaws</i> THOMAS A. NONDAHL t.nondahl@ieee.org	<i>Electronic Communication</i> CLIFTON OERTLI coertli@neieng.com	<i>Financial Planning</i> DONALD S. ZINGER d.zinger@ieee.org	<i>Intersociety Cooperation</i> TOMY SEBASTIAN t.sebastian@ieee.org	<i>Long Range Planning</i> BLAKE LLOYD BlakeLloyd@ieee.org	<i>Nominating</i> THOMAS A. NONDAHL t.nondahl@ieee.org

Members-at-Large

JIN-WOO AHN jwahn@star.kyungnung.ac.kr	A. J. MARQUES CARDOSO ajmcardoso@ieee.org	J. J. DAI jjd@etap.com	RICHARD LUKASZEWSKI ralukaszewski@ra.rockwell.com
TAMAS RUZSANYI tamas.ruzsanyi@ieee.org	MICHAEL WILLIAMS mikew@bgenergy.com	LONGYA XU xu.12@osu.edu	

Note: Additional information about the organization of the Industry Applications Society may be found on the IAS Web site, <http://www.ieee.org/ias/>

IEEE Officers

GORDON W. DAY, <i>President</i>	MICHAEL R. LIGHTNER, <i>Vice President, Educational Activities</i>
PETER W. STAECKER, <i>President-Elect</i>	DAVID A. HODGES, <i>Vice President, Publication Services and Products</i>
CELIA L. DESMOND, <i>Secretary</i>	HOWARD E. MICHEL, <i>Vice President, Member and Geographic Activities</i>
HAROLD L. FLESCHER, <i>Treasurer</i>	STEVE M. MILLS, <i>President, Standards Association</i>
MOSHE KAM, <i>Past President</i>	FREDERICK C. MINTZER, <i>Vice President, Technical Activities</i>
	JAMES M. HOWARD, <i>President, IEEE-USA</i>
J. KEITH NELSON, <i>Director, Division II</i>	

IEEE Executive Staff

DR. E. JAMES PRENDERGAST, <i>Executive Director & Chief Operating Officer</i>	ALEXANDER PASIK, <i>Information Technology</i>
THOMAS SIEGERT, <i>Business Administration</i>	PATRICK MAHONEY, <i>Marketing</i>
MATTHEW LOEB, <i>Corporate Activities</i>	CECELIA JANKOWSKI, <i>Member and Geographic Activities</i>
DOUGLAS GORHAM, <i>Educational Activities</i>	ANTHONY DURNIAK, <i>Publications Activities</i>
EILEEN LACH, <i>General Counsel & Corporate Compliance Officer</i>	KONSTANTINOS KARACHALIOS, <i>Standards Activities</i>
BETSY DAVIS, <i>SPHR, Human Resources</i>	MARY WARD-CALLAN, <i>Technical Activities</i>
CHRIS BRANTLEY, <i>IEEE-USA</i>	

IEEE Periodicals

Transactions/Journals Department

Staff Director: FRAN ZAPPULLA

Editorial Director: DAWN MELLEY *Production Director:* PETER M. TUOHY
Managing Editor: JEFFREY E. CICHOCKI *Senior Editor:* KEITH H. EDICK

IEEE TRANSACTIONS ON INDUSTRY APPLICATIONS (ISSN 0093-9994) is published bimonthly by the Institute of Electrical and Electronics Engineers, Inc. Responsibility for the contents rests upon the authors and not upon the IEEE, the Society/Council, or its members. **IEEE Corporate Office:** 3 Park Avenue, 17th Floor, New York, NY 10016-5997. IEEE Operations Center: 445 Hoes Lane, Piscataway, NJ 08854-4141. **NJ Telephone:** +1 732 981 0060. **Price/Publication Information:** Individual copies: IEEE Members \$20.00 (first copy only), non-members \$174.00 per copy. (Note: Postage and handling charge not included.) Member and nonmember subscription prices available upon request. **Copyright and Reprint Permissions:** Abstracting is permitted with credit to the source. Libraries are permitted to photocopy for private use of patrons, provided the per-copy fee indicated in the code at the bottom of the first page is paid through the Copyright Clearance Center, 222 Rosewood Drive, Danvers, MA 01923. For all other copying, reprint, or republication permission, write to Copyrights and Permissions Department, IEEE Publications Administration, 445 Hoes Lane, Piscataway, NJ 08854-4141. Copyright © 2012 by the Institute of Electrical and Electronics Engineers, Inc. All rights reserved. Periodicals Postage Paid at New York, NY and at additional mailing offices. **Postmaster:** Send address changes to IEEE TRANSACTIONS ON INDUSTRY APPLICATIONS, IEEE, 445 Hoes Lane, Piscataway, NJ 08854-4141. GST Registration No. 125634188. CPC Sales Agreement #40013087. Return undeliverable Canada addresses to: Pitney Bowes IMEX, P.O. Box 4332, Stanton Rd., Toronto, ON M5W 3J4, Canada. IEEE prohibits discrimination, harassment and bullying. For more information visit <http://www.ieee.org/nondiscrimination>. Printed in U.S.A.



Source details

IEEE Transactions on Industry Applications

Formerly known as: IEEE Transactions on Industry and General Applications

Scopus coverage years: from 1972 to Present

Publisher: IEEE

ISSN: 0093-9994 E-ISSN: 1939-9367

Subject area: Engineering: Industrial and Manufacturing Engineering Engineering: Electrical and Electronic Engineering Engineering: Control and Systems Engineering

Source type: Journal

CiteScore 2021 **9.7**

SJR 2021 **1.983**

SNIP 2021 **1.766**

[View all documents >](#)

[Set document alert](#)

[Save to source list](#) [Source Homepage](#)

[CiteScore](#) [CiteScore rank & trend](#) [Scopus content coverage](#)

Improved CiteScore methodology

CiteScore 2021 counts the citations received in 2018-2021 to articles, reviews, conference papers, book chapters and data papers published in 2018-2021, and divides this by the number of publications published in 2018-2021. [Learn more >](#)

CiteScore 2021

$$9.7 = \frac{25,630 \text{ Citations } 2018 - 2021}{2,643 \text{ Documents } 2018 - 2021}$$

Calculated on 05 May, 2022

CiteScoreTracker 2022

$$9.8 = \frac{26,547 \text{ Citations to date}}{2,721 \text{ Documents to date}}$$

Last updated on 05 April, 2023 • Updated monthly

CiteScore rank 2021

Category	Rank	Percentile
Engineering		
Industrial and Manufacturing Engineering	#25/338	92nd
Engineering		
Electrical and Electronic Engineering	#64/708	91st

[View CiteScore methodology >](#) [CiteScore FAQ >](#) [Add CiteScore to your site](#)

About Scopus

[What is Scopus](#)

[Content coverage](#)

[Scopus blog](#)

[Scopus API](#)

[Privacy matters](#)

Language

[日本語版を表示する](#)

[查看简体中文版本](#)

[查看繁體中文版本](#)

[Просмотр версии на русском языке](#)

Customer Service

[Help](#)

[Tutorials](#)

[Contact us](#)

ELSEVIER

[Terms and conditions ↗](#) [Privacy policy ↗](#)

Copyright © Elsevier B.V. ↗. All rights reserved. Scopus® is a registered trademark of Elsevier B.V.

We use cookies to help provide and enhance our service and tailor content. By continuing, you agree to the use of cookies ↗.





Document details - A dual five-phase space-vector modulation algorithm based on the decomposition method

1 of 1

Export Download More... >

IEEE Transactions on Industry Applications
Volume 48, Issue 6, 2012, Article number 6340331, Pages 2110-2120

A dual five-phase space-vector modulation algorithm based on the decomposition method(Article)

Jones, M., Nyoman Wahyu Satiawan, I., Bodo, N., Levi, E.

School of Engineering, Technology and Maritime Operations, Liverpool John Moores University, Liverpool, L3 3AF, United Kingdom

Abstract

Open-end winding variable speed drives with dual-inverter supply have been extensively investigated for various applications, including series hybrid power-trains and propulsion motors. The topology is simple to realize while offering a higher number of switching states without the need for capacitor voltage balancing algorithms, when compared to standard multilevel converters. The overwhelming majority of work is, however, restricted to the three-phase electric machinery. One of the reasons for this is that inclusion of a multiphase machine leads to exponential increase in the number of possible switching states, and so the design of a suitable space vector modulator (SVM) represents a considerable challenge. This paper considers a relatively simple SVM algorithm based on the decomposition of the three-level space vector decagon into a number of two-level decagons. The proposed modulation technique has the advantage of being relatively simple to implement. The drive produces multilevel load phase voltages with negligible low-order harmonic content. Despite the simplicity of the method, the quality of the output voltages is improved, compared to the previously proposed methods. The developed scheme is verified via detailed simulations and experiments using a five-phase induction machine under open-loop V/f control. © 1972-2012 IEEE.

Author keywords

Induction motor drives multiphase ac drives open-end winding space vector modulation

Indexed keywords

Engineering uncontrolled terms

AC drives Capacitor voltage balancing Decomposition methods Exponential increase
 Induction machines Induction motor drive Low order harmonics Modulation techniques
 Multi-level load Multilevel converter Multiphase machines Open-end windings
 Output voltages Phase voltage Propulsion motors Space Vector Space Vector Modulation
 Space vector modulators SVM algorithm Three-level V/f control

Engineering controlled terms:

Electric drives Electric inverters Electric machinery Induction motors Machinery
 Modulation Phase space methods Power converters Variable speed drives Winding

Engineering main heading:

Vector spaces

Funding details

Funding sponsor	Funding number	Acronym
Qatar Foundation		QF
Qatar National Research Fund		QNRF

Cited by 40 documents

Li, T., Ma, R., Bai, H.

A compare research on third harmonic current control for five-phase permanent magnet synchronous motor | 五相永磁同步电机三次谐波电流控制比较研究

(2021) *Xibei Gongye Daxue Xuebao/Journal of Northwestern Polytechnical University*

Jayakumar, V., Chokkalingam, B., Munda, J.L.

A comprehensive review on space vector modulation techniques for neutral point clamped multi-level inverters

(2021) *IEEE Access*

Balakrishna, J., Reddy, T.B., Kumar, M.V.

Discontinuous PWM Techniques to Eliminate Over-Charging Effects in Four-Level Five-Phase Induction Machine Drives

(2021) *Lecture Notes in Electrical Engineering*

View details of all 40 citations

Inform me when this document is cited in Scopus:

Set citation alert > Set citation feed >

Related documents

Find more related documents in Scopus based on:

Authors > Keywords >

SciVal Topic Prominence

Topic:

Prominence percentile:

A Dual Five-Phase Space-Vector Modulation Algorithm Based on the Decomposition Method

Martin Jones, I. Nyoman Wahyu Satiawan, Nandor Bodo, *Student Member, IEEE*, and Emil Levi, *Fellow, IEEE*

Abstract—Open-end winding variable speed drives with dual-inverter supply have been extensively investigated for various applications, including series hybrid power-trains and propulsion motors. The topology is simple to realize while offering a higher number of switching states without the need for capacitor voltage balancing algorithms, when compared to standard multilevel converters. The overwhelming majority of work is, however, restricted to the three-phase electric machinery. One of the reasons for this is that inclusion of a multiphase machine leads to exponential increase in the number of possible switching states, and so the design of a suitable space vector modulator (SVM) represents a considerable challenge. This paper considers a relatively simple SVM algorithm based on the decomposition of the three-level space vector decagon into a number of two-level decagons. The proposed modulation technique has the advantage of being relatively simple to implement. The drive produces multilevel load phase voltages with negligible low-order harmonic content. Despite the simplicity of the method, the quality of the output voltages is improved, compared to the previously proposed methods. The developed scheme is verified via detailed simulations and experiments using a five-phase induction machine under open-loop V/f control.

Index Terms—Induction motor drives, multiphase ac drives, open-end winding, space vector modulation.

I. INTRODUCTION

MULTILEVEL and multiphase voltage source inverters (VSIs) have been attracting increasing research interest recently due to their ability to overcome voltage and current limitations of power semiconductors and their inherent ability to tolerate faults [1]–[3]. Multilevel inverters are considered as a topology which enhances the quality of the output voltage waveform, reduces dv/dt , and enables the construction of a high power converter without the problem of switching series-connected semiconductor devices. There are numerous configurations of multilevel converters, the main ones being the neutral point clamped (NPC), the flying capacitor, and the cascaded converters [4].

The open-end winding topology, originally described in [5], can be considered as an alternative approach to create multilevel

load phase voltage waveforms. The equivalence of the topology with a two-level inverter on each side of the stator winding and three-level or four-level single-sided supplied drive (depending on the dc-bus voltage ratio) is shown in terms of performance and created multilevel load phase voltages in [6] for three-phase drives. The open-end topology has the advantages that the additional diodes used in the NPC VSI are not needed, leading to a saving in the overall number of components. Furthermore, the issue of proper capacitor voltage balancing does not exist if the supply is two level at each winding side. Typically, three-phase VSIs are utilized. It has been suggested in the literature that such drives may, in the future, offer an alternative supply solution in applications such as EVs/HEVs [7]–[9], electric ship propulsion [10], and rolling mills [11]. Recent research efforts have been directed toward investigating the potential of this supply configuration in renewable electric energy systems [12] and fault-tolerant drives [13].

Due to their well-known advantages [1], multiphase drives have also been considered for similar applications as the multilevel drives. As a consequence, some researchers have begun investigating the benefits of combining both technologies [14]–[24]. Recently, some research effort has been directed toward the multiphase open-end winding topology [14]–[18]. An asymmetrical six-phase induction motor drive has been developed in [14], [15]. In [14], the supply is provided by means of two isolated two-level six-phase VSIs. The goal was in essence low-order harmonic elimination/reduction rather than the multilevel operation, so that the dual converter is not operated in multilevel mode. The topology discussed in [15] uses four three-phase two-level inverters, with four isolated dc sources, to prevent circulation of zero sequence currents. The space vector modulator (SVM) control is performed in essence independently for the two three-phase windings, using the nearest three vectors approach in conjunction with three-level inverter. The work is focused on controlling the power sharing between the four converters. The five-phase configuration has been examined in [16], [17] and a suitable SVM algorithm proposed. In [18], the SVM algorithm of [17] is extended to the seven-phase structure.

The remaining literature is primarily centered on the five-phase NPC VSI fed drive [19]–[23]. The first SVM techniques for multiphase VSIs were based on the simple extension of the three-phase multilevel SVM approaches, so that only the three vectors, nearest to the reference, were utilized [19]. As a consequence, only the first plane of the multiphase system is controlled. In principle, the number of applied vectors must equal the number of phases [1]. Hence, numerous low-order harmonics are generated, which map into the second plane. A

Manuscript received December 30, 2011; revised March 20, 2012; accepted April 1, 2012. Date of publication October 25, 2012; date of current version December 31, 2012. Paper 2011-IPCC-795.R1, approved for publication in the IEEE TRANSACTIONS ON INDUSTRY APPLICATIONS by the Industrial Power Converter Committee of the IEEE Industry Applications Society. This work was supported by NPRP Grant 4-152-02-053 from the Qatar National Research Fund (a member of the Qatar Foundation). The statements made herein are solely the responsibility of the authors.

The authors are with the School of Engineering, Technology and Maritime Operations, Liverpool John Moores University, Liverpool, L3 3AF, U.K. (e-mail: M.Jones2@ljmu.ac.uk; I.N.Satiawan@2008.ljmu.ac.uk; N.bodo@2009.ljmu.ac.uk; e.levi@ljmu.ac.uk).

Color versions of one or more of the figures in this paper are available online at <http://ieeexplore.ieee.org>.

Digital Object Identifier 10.1109/TIA.2012.2226422

SVM method, which controls both planes, has been developed in [20] for the three-level NPC VSI fed five-phase drive, and it was extended to the seven-phase case in [21]. The SVM method is complicated, particularly the sector identification, since each 36° sector is partitioned into ten subsectors. A different approach to the SVM of multilevel multiphase systems is given for a general case of an m -level, n -phase VSI in [22]. The algorithm is based on the considerations of the multidimensional (n -dimensional) space and therefore does not include decomposition of the n -dimensional space into 2-D planes. A somewhat similar method, in the sense that decomposition into 2-D planes is not utilized, is the one in [23], where a multiphase multilevel PWM is developed using n single-leg modulators. Level-shifted and phase-shifted carrier-based PWM methods have recently been applied to the five-phase open-end topology in [24], where it was shown that PWM methods developed for NPC converters can be applied to the five-phase open-end topology.

This paper develops further the modulation method originally proposed in [25] for a five-phase open-end winding drive, based on two two-level inverters. The SVM algorithm is based on the decomposition of the three-level space vector decagon into a number of two-level decagons. A similar idea has been proposed in [26] for a three-phase NPC inverter and in [27] for a three-phase open-end winding drive. In the case of the five-phase open-end winding drive, the situation is significantly more complicated since both 2-D planes have to be considered. It is shown here that the algorithm proposed in [26] can lead to an increase in the dc-link voltage of one of the inverters, over a small operating range, and a simple solution is suggested as a remedy. The proposed modulation strategy is verified for the first time using detailed simulations and a set of experiments. The results indicate that the method is capable of achieving the target fundamental while eliminating fully any low-order harmonic content in the output load phase voltage. Furthermore, the modulation method gives superior harmonic performance to the one given in [17].

The paper begins with a review of the five-phase two-level drive characteristics followed by a general description and mathematical model of the cascaded topology, including mapping of the space vectors into the 2-D planes. Next, the proposed modulation method is described. It is shown that due to the nature of the five-phase topology one of the inverters needs to be operated using so-called multi-frequency SVM [28] and the inverters must operate with slightly different dc-link voltages. Finally, simulation and experimental results verify the performance of the drive.

II. GENERAL PROPERTIES OF TWO-LEVEL FIVE-PHASE DRIVES

Prior to considering the SVM scheme for the open-end winding topology, it is beneficial to review the basic relationships which govern the performance of five-phase drives and the corresponding two-level SVM technique for a five-phase VSI. A five-phase machine can be modeled in two 2-D subspaces, so-called $\alpha - \beta$ and $x - y$ subspaces [1]. It can be shown that only current harmonic components which map into the $\alpha - \beta$ subspace develop useful torque and torque ripple, whereas those

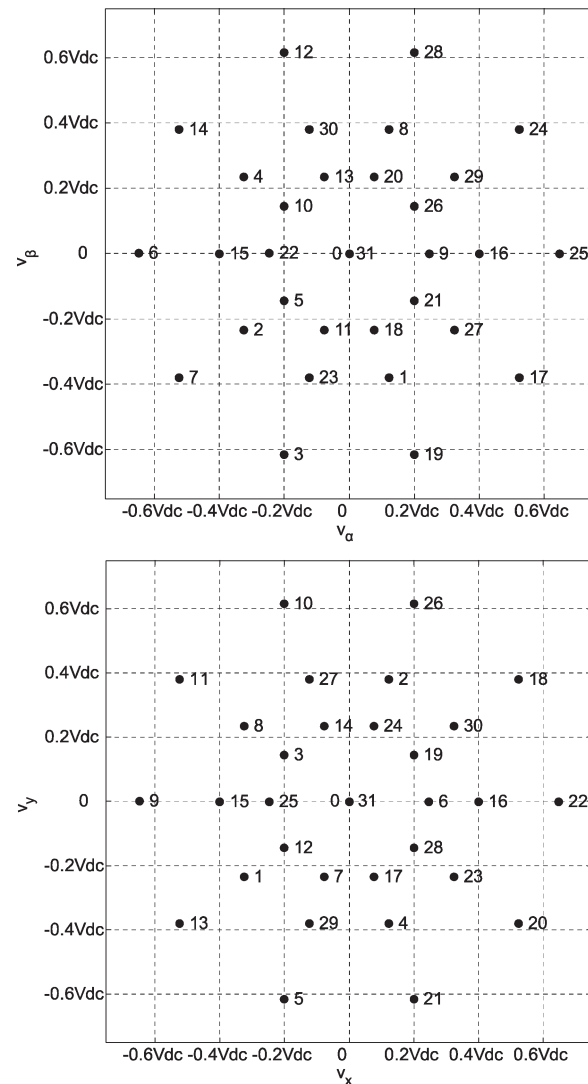


Fig. 1. Two-level five-phase VSI space vectors in the $\alpha - \beta$ and $x - y$ planes.

that map into the $x - y$ subspace do not contribute to the torque at all. A multiphase machine with near-sinusoidal magnetomotive force distribution presents extremely low impedance to all non-flux/torque producing supply harmonics, and it is therefore mandatory that the supply does not generate such harmonics. What this means is that the design of a five-phase PWM strategy must consider simultaneously both 2-D subspaces, where the reference voltage, assuming pure sinusoidal references, is in the first plane while reference in the other plane is zero. Two-level five-phase inverters can generate up to $2^5 = 32$ voltage space vectors with corresponding components in the $\alpha - \beta$ and $x - y$ subspaces, as shown in Fig. 1. Space vectors are labeled with decimal numbers, which, when converted into binary code, reveal the values of the switching functions of each of the inverter legs. Active (non-zero) space vectors belong to three groups in accordance with their magnitudes - small, medium and large space vector groups. The magnitudes are identified with indices s , m , and l and are given as, respectively, $|\underline{v}_s| = 4/5 \cos(2\pi/5)V_{dc}$, $|\underline{v}_m| = 2/5V_{dc}$, and $|\underline{v}_l| = 4/5 \cos(\pi/5)V_{dc}$. Four active space vectors are required

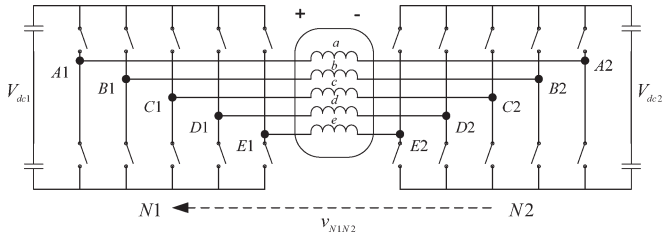


Fig. 2. Five-phase open-end winding topology.

to generate sinusoidal voltages [1]. In order to provide zero average voltage in the $x - y$ plane two neighboring large and two medium space vectors are selected [29]. It is shown in [30], [31] that the maximum peak value of the output fundamental phase-to-neutral voltage in the linear modulation region is $v^{h1\max} = 0.525V_{dc}$, resulting in the maximum modulation index, $M = 1.05$. Switching pattern is a symmetrical PWM with two commutations per inverter leg.

III. FIVE-PHASE OPEN-END WINDING TOPOLOGY

Fig. 2 illustrates the open-end winding structure, based on utilisation of two two-level five-phase VSIs. The two inverters are identified with indices 1 and 2. Inverter legs are denoted with capital letters, A, B, C, D, E and the negative rails of the two dc-links are identified as $N1$ and $N2$. Machine phases are labeled as a, b, c, d, e . Load phase voltage positive direction is with reference to the left inverter (inverter 1). Two isolated dc supplies are assumed so that the common mode voltage (CMV) v_{N1N2} is of non-zero value (the issue of CMV elimination is not addressed here). The resulting space vectors in dual-inverter supply mode will depend on the ratio of the two dc-link voltages. When the dc-link voltages are equal, i.e., $V_{dc1} = V_{dc2} = V_{dc}/2$, the resulting space-vector pattern is identical to the equivalent single-sided three-level supply. Using the notation of Fig. 2, load phase voltages of the stator winding can be given as

$$\begin{aligned} v_a &= v_{A1N1} + v_{N1N2} - v_{A2N2} \\ v_b &= v_{B1N1} + v_{N1N2} - v_{B2N2} \\ v_c &= v_{C1N1} + v_{N1N2} - v_{C2N2} \\ v_d &= v_{D1N1} + v_{N1N2} - v_{D2N2} \\ v_e &= v_{E1N1} + v_{N1N2} - v_{E2N2}. \end{aligned} \quad (1)$$

Space vectors of load phase voltages in the two planes are determined with

$$\begin{aligned} v_{\alpha-\beta} &= (2/5) (v_a + \underline{a}v_b + \underline{a}^2v_c + \underline{a}^3v_d + \underline{a}^4v_e) \\ \underline{v}_{x-y} &= (2/5) (v_a + \underline{a}^2v_b + \underline{a}^4v_c + \underline{a}^6v_d + \underline{a}^8v_e) \end{aligned} \quad (2)$$

where $\underline{a} = \exp(j2\pi/5)$. Using (1) and (2), one gets

$$\begin{aligned} v_{\alpha-\beta} &= \underline{v}_{\alpha-\beta(A1B1C1D1E1)} - \underline{v}_{\alpha-\beta(A2B2C2D2E2)} \\ \underline{v}_{x-y} &= \underline{v}_{x-y(A1B1C1D1E1)} - \underline{v}_{x-y(A2B2C2D2E2)} \end{aligned} \quad (3)$$

since $v_{N1N2}(1 + \underline{a} + \underline{a}^2 + \underline{a}^3 + \underline{a}^4) = 0$.

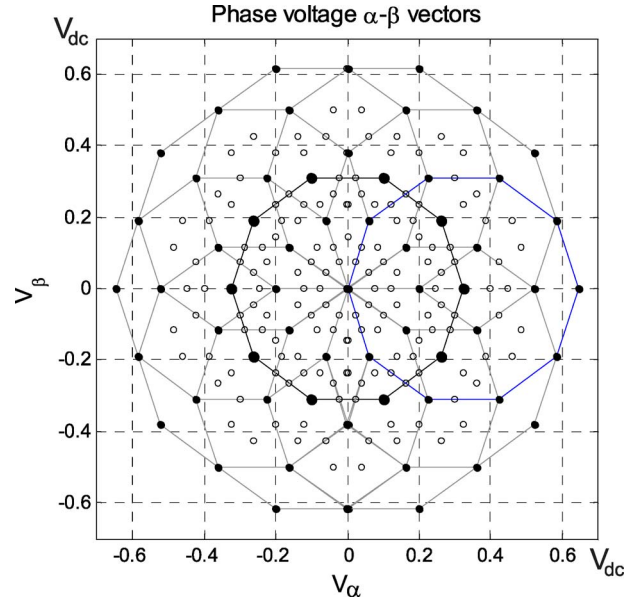


Fig. 3. Space-vector distribution of the dual-inverter supplied five-phase open-end topology in the $\alpha - \beta$ plane, $V_{dc1} = V_{dc2} = V_{dc}/2$.

In (3), the two space vectors on the right-hand sides of the two equations are corresponding voltage space vectors of the two five-phase two-level VSIs, which come in three different lengths already discussed in the previous section. Their combinations result in 211 voltage space vectors, produced by 1024 possible switching states [16]. These are illustrated in Fig. 3 for the $\alpha - \beta$ plane. Space-vector mapping into the $x - y$ plane follows the pattern that exists for a five-phase VSI, the largest vectors of the first plane map into the smallest vectors of the second plane and so on. A consequence of the greater number of voltage space vectors is an increased number of load phase voltage levels.

IV. PRINCIPLE OF THE PROPOSED ALGORITHM

Another consequence of the large number of switching states and space vectors is that the development of a suitable SVM strategy is challenging. The complexity of selecting the proper switching states for a given command voltage can be significantly reduced if the three-level space-vector decagon is decomposed into a number of two-level decagons as shown in Fig. 3. A similar approach was followed in [27] for the three-phase case. The center decagon comprises vectors which can be activated if one inverter is used up to half of the achievable maximum voltage with the other one locked in a zero vector state. As a consequence, the converter is in two-level mode of operation based on four active and zero vector application, as discussed in Section II and [29]. As can be seen in Fig. 3, the origins of the outer decagons are located on the outer vectors of the inner decagon, denoted by the larger dots in Fig. 3, which correspond to the outermost vectors and switching states given in Fig. 1. In the case of the three-phase topology [27], operation in the outer region (outer hexagon) is achieved when one inverter operates with a single voltage space vector applied (the nearest one to the reference), and the second inverter

is modulated using the standard three-phase two-level SVM technique. Let the applied vector for one inverter be \underline{v}_i , and let the reference be \underline{v}^* . Here, \underline{v}_i is the vector produced by the inverter that is the nearest to the reference, and \underline{v}^* exceeds, in magnitude, maximum voltage realizable with one inverter. The reference for the other inverter is then set as

$$\underline{v}^{**} = -(\underline{v}^* - \underline{v}_i). \quad (4)$$

In other words, when the magnitude of the reference voltage exceeds the maximum value obtainable with one inverter, one inverter is operated in six-step (i.e., ten-step) mode, while the second inverter is modulated in the standard way.

It is well known that operation of a five-phase inverter in ten-step mode, without a controllable dc-link voltage, leads to uncontrollable fundamental output voltage magnitude and unwanted low-order harmonics, which, for the leg voltage of inverter 1, can be expressed as a Fourier series as

$$v_{leg} = \frac{2}{\pi} V_{dc1} \left[\sin \omega t + \frac{1}{3} \sin 3\omega t + \frac{1}{5} \sin 5\omega t + \frac{1}{7} \sin 7\omega t \dots \right]. \quad (5)$$

In a five-phase system, harmonics of the order $10k \pm 1$ ($k = 0, 1, 2, 3, \dots$) map onto the torque/flux producing subspace, $\alpha - \beta$, while harmonics of the order $10k \pm 3$ map into the $x - y$ subspace. They do not produce any useful torque/flux and simply lead to large unwanted loss-producing currents. The large currents are a consequence of the relatively small impedance presented in $x - y$ plane. $10k \pm 5$ are zero-sequence components. This leads to the requirement that the second inverter must be able to not only control the fundamental but also eliminate the unwanted low-order harmonics, which are produced by applying only the large vector in the $\alpha - \beta$ plane from one inverter. This causes unwanted harmonics in both planes since a large vector has a corresponding non-zero value in the second, $x - y$ plane (Fig. 1). In order to achieve this objective, the second inverter modulation scheme will need to operate in both the $\alpha - \beta$ and the $x - y$ planes, since the references for the second inverter can be given as

$$\begin{aligned} v_{\alpha}^{**} &= -(v_{\alpha}^* - v_{i(\alpha)}) & v_{\beta}^{**} &= -(v_{\beta}^* - v_{i(\beta)}) \\ v_x^{**} &= v_{i(x)} & v_y^{**} &= v_{i(y)}. \end{aligned} \quad (6)$$

Here, $i = 1 \dots 10$ stands for the large vector of the first VSI. A SVM, which achieves simultaneous control in both the $\alpha - \beta$ and $x - y$ planes, was developed in [28] in order to control multiphase multi-motor drive systems. A schematic illustration of the SVM process is shown in Fig. 4. This SVM method utilizes two two-level five-phase SVMs, as described in Section II. Each space-vector modulator operates in a separate plane. The duty cycles from the SVMs are summed according to the phase transposition rule [32]. The phase transposition [32] enables the lower five-phase SVM to operate in the $x - y$ plane. This further simplifies the algorithm since identification of the sector, dwell time calculation and the vector look-up table are identical for both modulators.

As a result of the proposed modulation technique for the open-end winding configuration, the converter operates using

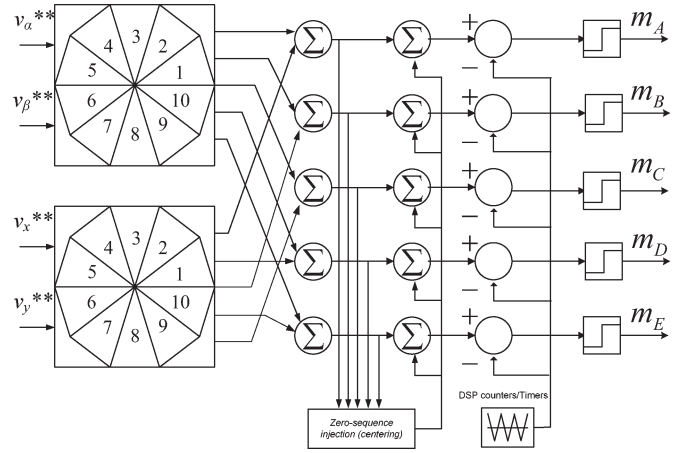


Fig. 4. Signal flow of the five-phase multi-frequency space-vector modulator.

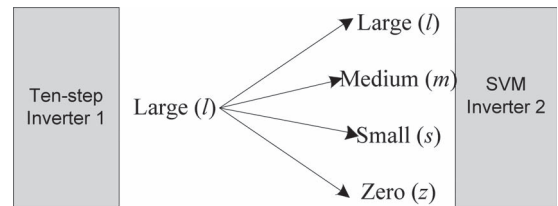


Fig. 5. Five-phase dual-inverter switching combinations.

only the large vectors from one inverter and any combination of vectors from the other inverter, as illustrated in Fig. 5. This reduces the number of switching states to 342 (320 of these are the states met when both inverters operate, while 22 states are those that are encountered when only one inverter operates). The 342 switching states produce 151 vectors in the $\alpha - \beta$ and $x - y$ planes, as shown in Fig. 6. It can be seen that no large vectors are produced in the $x - y$ plane. Taking into account the number of space vectors and (1), the maximum number of load phase voltage levels is 15. A signal flow diagram of the complete space-vector modulation scheme is presented in Fig. 7(a). When $M < 0.525$, the switches in Fig. 7(a) are opened (in the upper position), meaning that the ten-step inverter is locked, with all upper or lower switches on, (i.e., so-called zero vector is applied), thus forming a star connection and the machine is supplied in single-sided mode. The second inverter is operated as a two-level inverter according to the SVM method outlined in Section II and discussed in detail in [29].

It is interesting to note that the two-level multiphase SVM method employs the same space vectors for the same dwell-times as one carrier-based PWM method [29] and thus gives the same results in terms of phase and line-to-line voltages. This equivalent carrier-based PWM method is the one with offset injection (i.e., zero-sequence signal injection), defined as $v_{zs} = -0.5(\max\{v_j^*\} + \min\{v_j^*\})$, $j = a, b, c, d, e$. Therefore, it can be concluded that the multi-frequency two-level modulator of Fig. 4 may be replaced with a carrier-based approach. Such an approach is shown in Fig. 7(b). It follows that the simulation and experimental results presented in this paper for the SVM are equally applicable to the carrier-based two-level modulation method with offset injection.

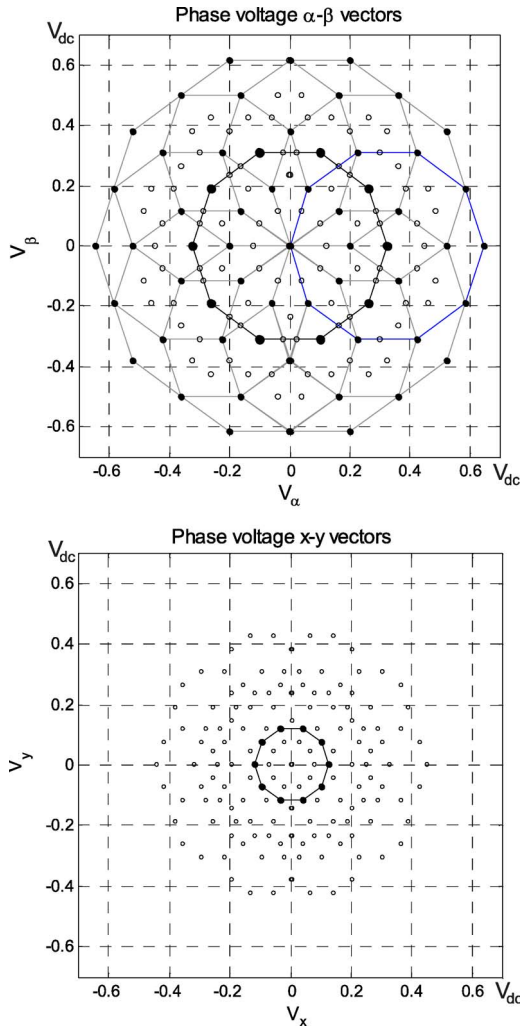


Fig. 6. Decomposed SVM space-vector distribution of the dual-inverter supplied open-end winding five-phase topology, in the $\alpha - \beta$ and $x - y$ planes.

V. DC-LINK VOLTAGES

For clarity, it is beneficial to define the modulation index of the space vector-modulated inverter as $M_2 = v^{**}/(0.5V_{dc2})$. Only inverter 2 is operational up to the point when $M = 0.525 (M_2 = 1.05)$. Hence, the converter operates in two-level mode, since inverter 1 is not engaged and is locked in a zero switching state 11111 or 00000, forming a neutral point. It is worth noting that the converter output is still significantly improved compared to the equivalent two-level single-sided configuration since the inverter is switching across the load half of the equivalent two-level converter's dc-link voltage. When $M > 0.525$, the second inverter operates in ten-step mode. In this operating regime, the space vector-modulated inverter will output the difference between the voltages created by the ten-step mode inverter and the reference. Since the output fundamental voltage of the ten-step inverter is fixed, there is a narrow band of modulation indices ($0.525 < M \leq 0.637$) where the fundamental output voltage of the ten-step inverter is greater than the reference voltage. Therefore, in this operating region, the SVM inverter acts to decrease the fundamental created by the ten-step inverter. At these modulation indices, all the power is supplied by the ten-step inverter, and what is

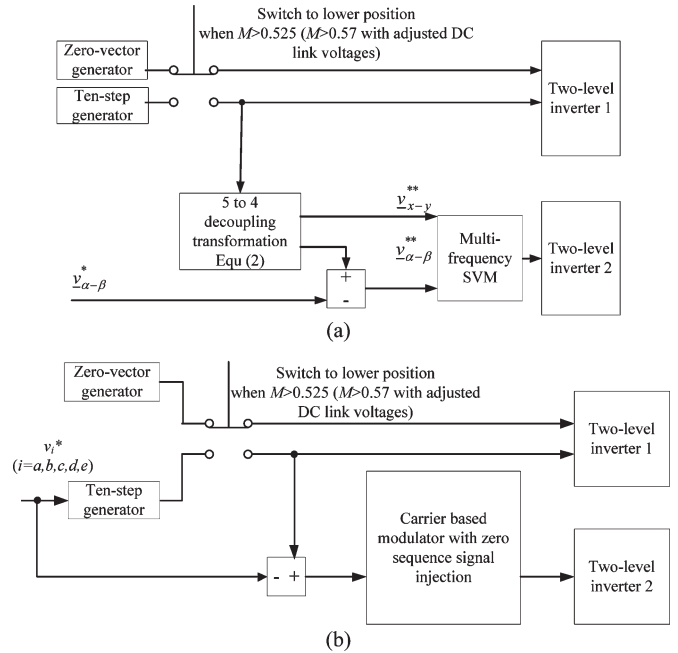


Fig. 7. Signal flow of the decomposition method using SVM modulator (a) or a carrier-based modulator (b).

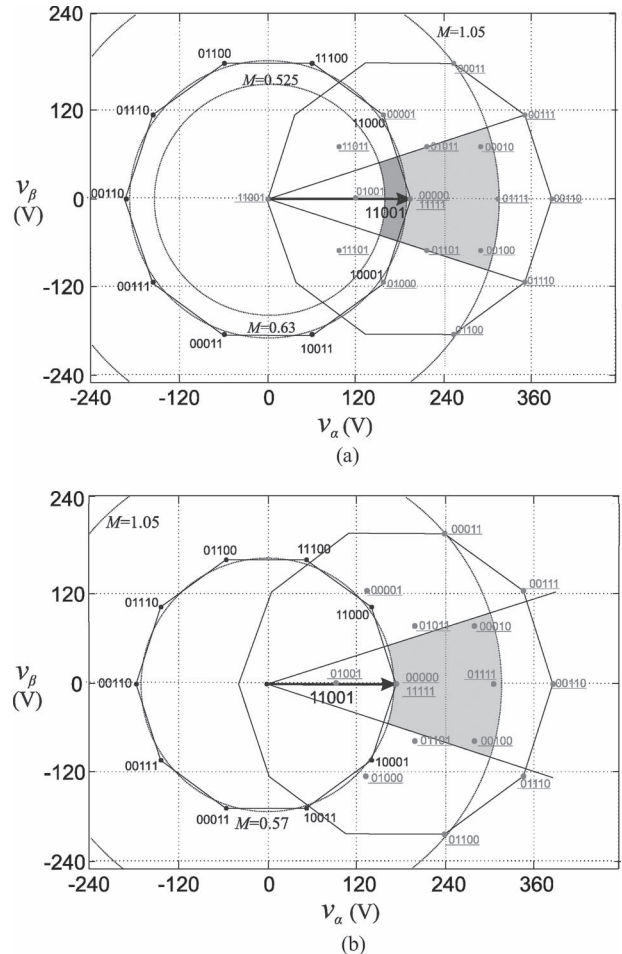


Fig. 8. Operating regions for system with equal 300-V dc-link voltages (a) and adjusted dc-link voltages (b).

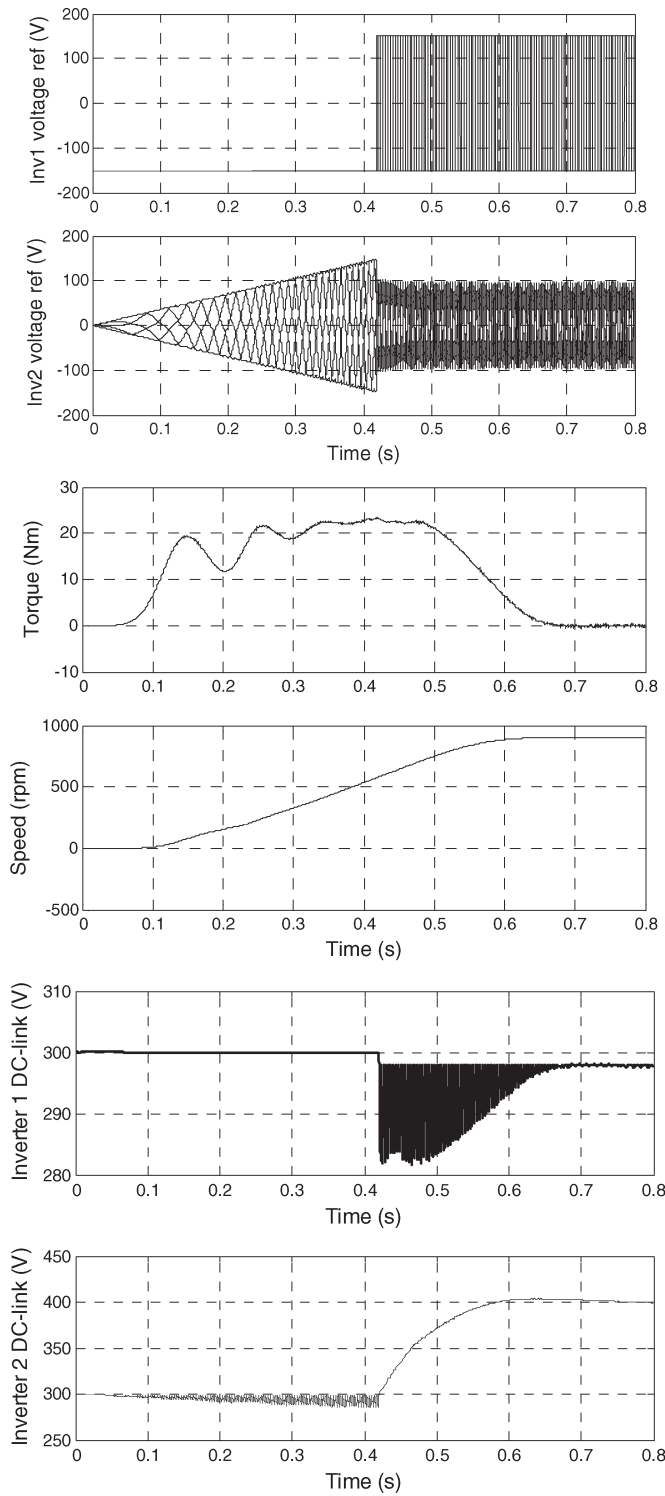


Fig. 9. Acceleration to 30 Hz with equal dc-link voltages: Inverter references, torque, speed response, and inverter dc-link voltages.

not consumed by the load is absorbed by the SVM inverter. If there is no regenerative rectifier on the side of the SVM inverter, its dc-link capacitor voltage will raise until the braking chopper is activated, and the energy is dissipated. Fig. 8(a) depicts the switching states used when the large vector 11001 is applied by the ten-step inverter along with the reference circular path for the relevant modulation indices. $M = 1.05$ is the maximum modulation index, $M = 0.525$ is half of the

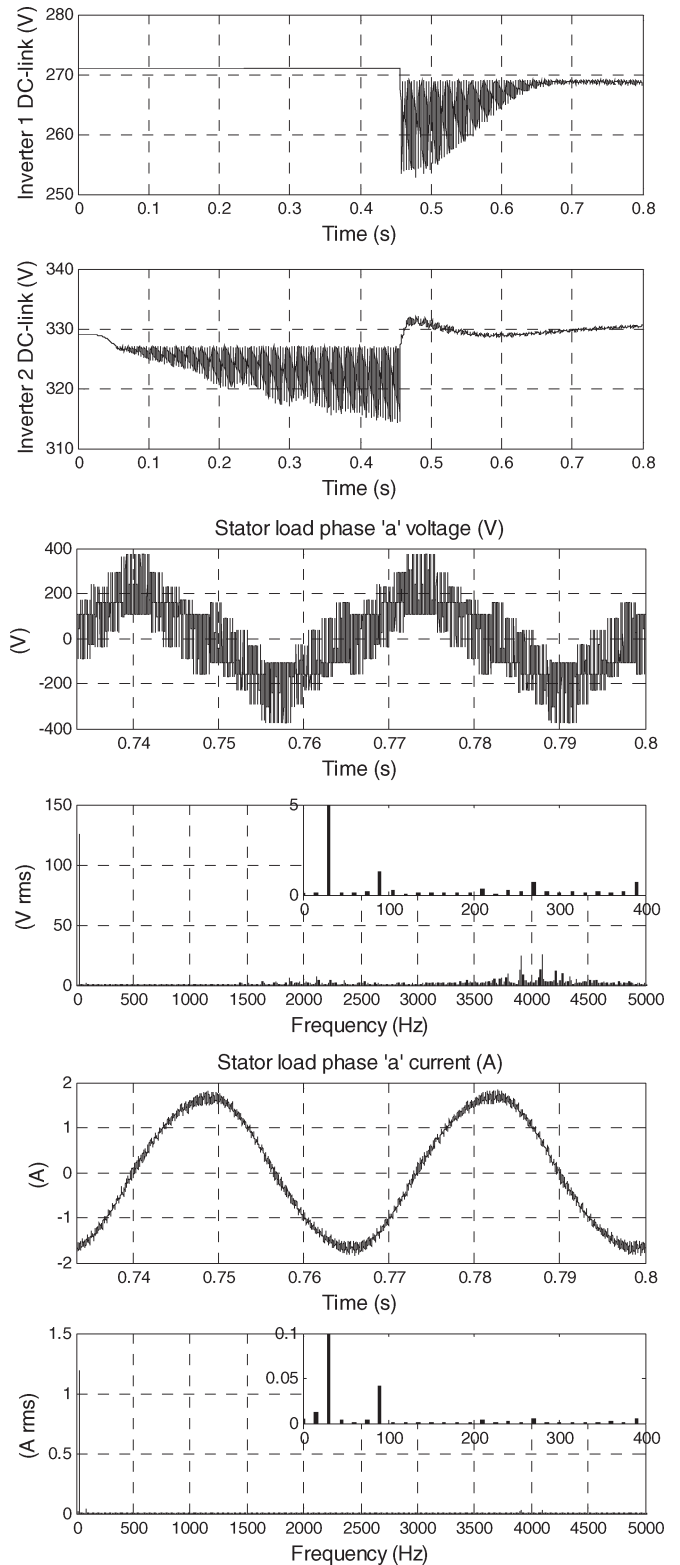


Fig. 10. Acceleration to 30 Hz with adjusted dc-link voltages according to (10) and (11): Inverter dc-link voltages, machine phase “a” voltage and stator phase “a” current waveforms and spectra.

maximum modulation index, the point at which the ten-step inverter starts to operate, and the lower boundary where the dc-link voltage increase begins. $M = 0.637$ (i.e., $2/\pi$) coincides with the magnitude of the fundamental of the ten-step inverter and is the upper boundary of dc-link voltage increase after

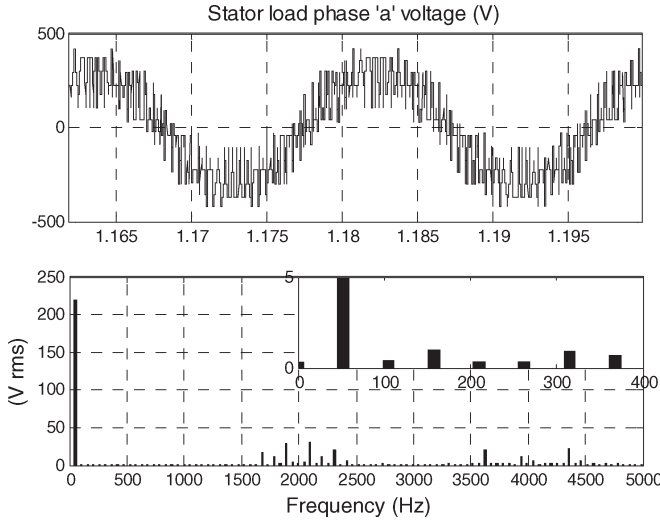


Fig. 11. Operation at $M = 1.05$, with adjusted dc-link voltages: Machine phase “a” voltage waveform and spectrum.

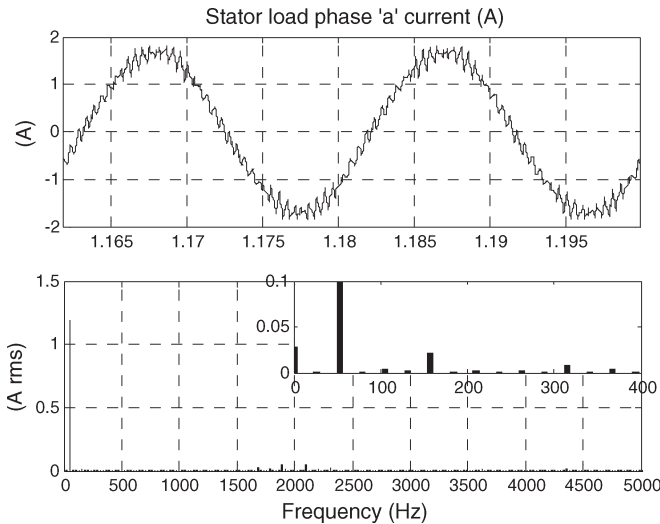


Fig. 12. Operation at $M = 1.05$, with adjusted dc-link voltages: Machine stator phase “a” current waveform and spectrum.

which no further increase is seen. The black dots in Fig. 8 are the vectors applied by the ten-step inverter, while the gray dots with underlined binary numbers are the vectors applied during the operation of both inverters. The increase is strongly dependent on the inductive part of the load impedance and can be substantial, leading to activation of the dynamic brake in the SVM inverter. One way to prevent this issue is to adjust the dc-link voltage ratio in such a way that the first harmonic of the ten-step inverter output equals the fundamental generated by the SVM inverter when at maximal modulation index, when operated on its own

$$v_1^{h1} = v_2^{h1 \max}. \tag{7}$$

The maximum achievable fundamental for a five-phase two-level SVM inverter is given with [29]

$$v_2^{h1 \max} = \frac{V_{dc2}}{2 \cos(\pi/10)}. \tag{8}$$

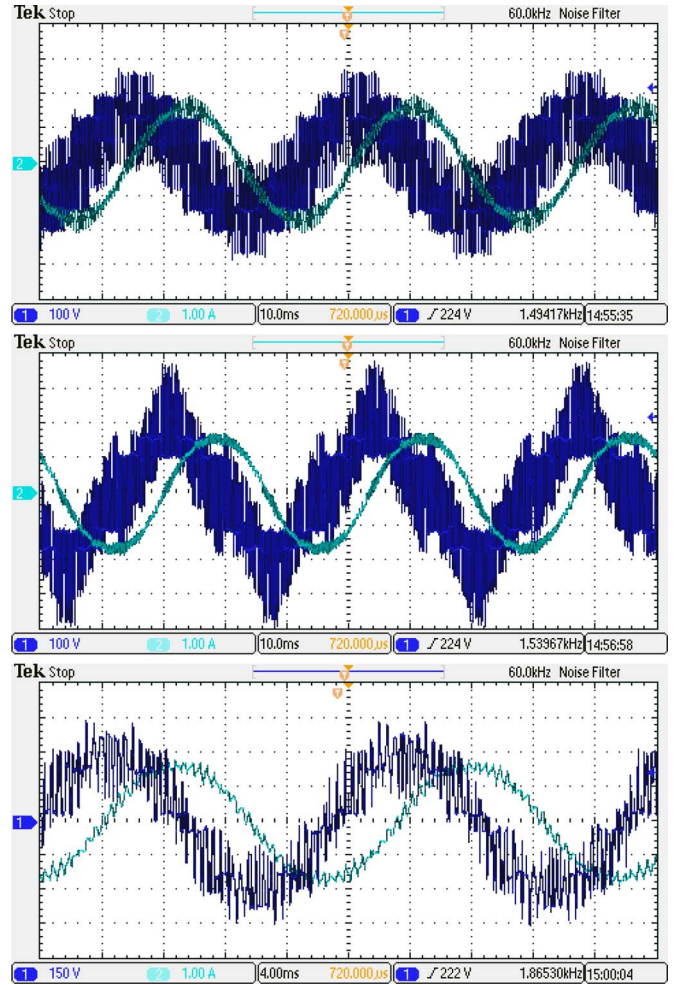


Fig. 13. Oscilloscope recordings of load phase voltage and current waveforms at $M = 0.55$ (top), $M = 0.6$ (middle), and $M = 1.05$ (bottom).

The fundamental voltage of the ten-step inverter is from (5)

$$v_1^{h1} = \frac{2}{\pi} V_{dc1} \tag{9}$$

Setting $V_{dc} = V_{dc1} + V_{dc2} = 600$ V to give the equivalent of single-sided three-level supply with a 600-V dc-link and taking into account (7)–(9), the required values for the individual inverter dc-link voltages are:

$$V_{dc1} = \frac{600}{1 + 4 \cos(\pi/10) / \pi} = 271.38 \text{ V} \tag{10}$$

$$V_{dc2} = \frac{600}{1 + \pi/4 \cos(\pi/10)} = 328.62 \text{ V}. \tag{11}$$

The highest achievable peak fundamental of the SVM inverter is

$$v_2^{h1 \max} = v_1^{h1} = \frac{600}{2 \cos(\pi/10) + \pi/2} = 172.76 \text{ V} \tag{12}$$

which corresponds to the modulation index $M = 0.57$. This means that the SVM inverter will operate alone up to $M = 0.57 (M_2 = 1.05)$. When $M > 0.57$ the ten-step inverter will operate as well. The adjustment of the dc-link voltages obviously leads to a somewhat different layout of the space

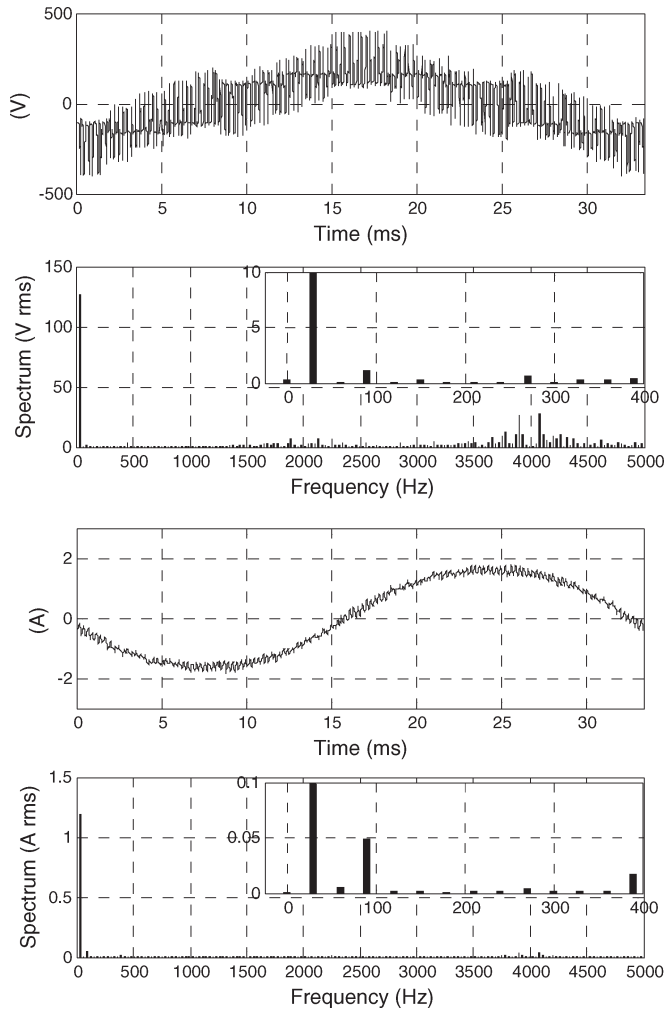


Fig. 14. Load phase voltage (top) and current (bottom) waveforms and spectra at $M = 0.6$.

vectors of the open-end winding converter, as shown in Fig. 8(b) for the case when the ten-step inverter applies the vector 11001. It can be seen that, although the SVM inverter applies the same switching states as in Fig. 8(a), the operating regions have changed, and the small region where the SVM inverter dc-link voltage is boosted has disappeared.

VI. SIMULATION VERIFICATION

In order to verify the converter’s performance, a series of detailed simulations were undertaken using the PLECS environment. Initially, the dc-link voltage of each inverter is 300 V ($V_{dc1} = V_{dc2} = V_{dc}/2$), the switching frequency of the modulated inverter is 2 kHz, and the implemented dead time is 6 μ s. The IGBT and diode models include an on-state resistance of 10 m Ω . The drive is operated in open-loop V/f mode. The voltage reference profile is such that the supply frequency of the machine is ramped from zero to 50 Hz in 0.8 s. At the operating frequency of 50 Hz the modulation index $M = 1$ is reached. Voltage boost is not included. The machine parameters are $L_{\gamma s} = 45$ mH, $L_{\gamma r} = 15$ mH, $L_m = 515$ mH, $R_r = 3$ Ω and $R_s = 3$ Ω and are those of the induction machine used further on in the experiments. First, acceleration of the drive

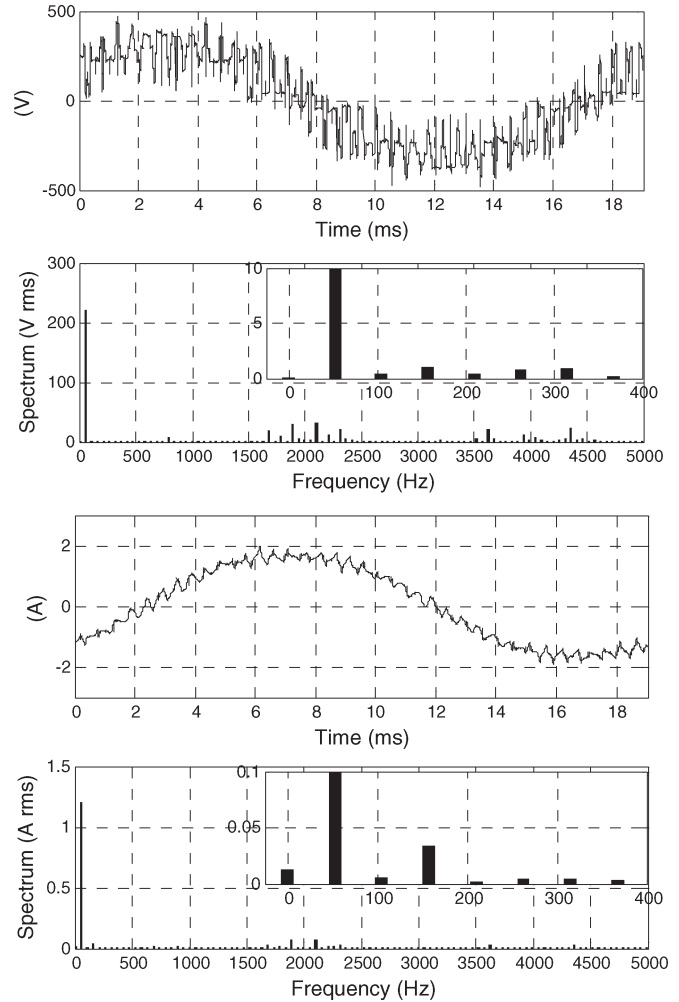


Fig. 15. Load phase voltage (top) and current (bottom) waveforms and spectra at $M = 1.05$.

from standstill to 900 rpm (30 Hz) is examined. Fig. 9 shows the developed torque and speed, the dc-link voltages, and the leg voltage references of the inverters. The dc-link voltage of the SVM inverter experiences a considerable increase. It can be seen that the increase coincides with the activation of the ten-step inverter (inverter 1) and is therefore a consequence of the excessive fundamental provided by the ten-step inverter.

Next, the individual inverter dc-link voltages are adjusted according to (10) and (11), and the simulation is re-run. The inverter references and machine torque response are similar to those already presented and are hence not given. Fig. 10 shows the dc-link voltage of the inverters, the steady-state machine phase “a” voltage and current waveforms and spectra. Clearly, the adjusted dc-link voltage setting has prevented the rise in dc-link voltage. The load phase voltage shows the converter operating in multilevel mode. The voltage and current spectra show a small amount of low-order harmonic content, predominantly the third. It is shown in [33], [34] that these harmonics are a consequence of the dead time and can be eliminated by a suitable closed-loop current control method. In other words, the low-order harmonics are not a direct result of the modulation method. Figs. 11 and 12 present the stator phase “a” voltage and current waveforms and spectra, respectively, for the case when

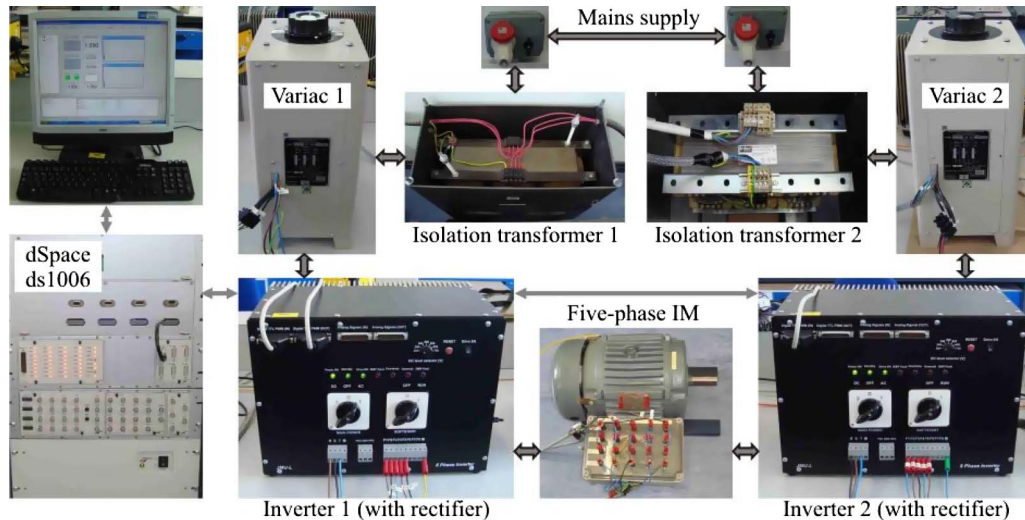


Fig. 16. Experimental setup.

$M = 1.05$ (maximum). The load phase voltage and current contain again a small amount of low-order harmonics and the fundamental magnitude matches the reference.

VII. EXPERIMENTAL VERIFICATION

The experimental results are obtained using two custom built five-phase two-level VSIs which utilize Infineon's FS50R12KE3 IGBTs. A four-pole five-phase induction motor is connected to the converter. Each stator phase consists of two half-windings, which can be connected in series or in parallel. In this paper, the half-windings are series connected. Parameters of this motor have been used in the simulation study of Section VII. The inverters are controlled using a dSPACE DS1006 processor board. The dSPACE module is connected to the VSIs via a dSPACE DS5101 digital waveform unit. The dc-link voltages are created for the two inverters of the open-end topology by using two isolation transformers, to isolate the mains supply, and variacs to adjust the voltage according to (10) and (11). The switching frequency of the SVM inverter is 2 kHz, and the inverter dead time is 6 μ s. The motor is controlled in open-loop V/f mode with the maximum modulation index ($M = 1.05$) being reached when the fundamental frequency is 52.5 Hz.

The waveforms are obtained using a Tektronix MSO 2014 Mixed Signal Oscilloscope. The machine phase "a" voltage is obtained using a Tektronix P5205A High Voltage Differential Probe, while the current waveform on channel 2 is obtained using a Tektronix TCP0030 Current Probe. Oscilloscope screen shots, showing the machine phase "a" voltage and current, are presented in Fig. 13 for operation when $M = 0.55$, $M = 0.6$ and $M = 1.05$. It can be seen that the converter operates in two-level mode when $M = 0.55$, as evidenced by the nine levels in the load phase voltage. When $M = 0.6$, the ten-step inverter is operational, and the converter operates in multilevel mode. Operation at $M = 1.05$ produces the maximum number of load phase voltage levels.

Figs. 14 and 15 depict the voltage and current waveforms and their associated spectra for the case when $M = 0.6$ and

$M = 1.05$, respectively. The FFTs of the load phase voltage and currents are obtained by measuring the load phase voltages and currents in 125 000 points. The resolution of the waveforms obtained in this way enables processing by Matlab to calculate the spectra. A good agreement between simulations and experiments can be observed by comparing Figs. 10–12 with Figs. 14 and 15. The voltage and current waveforms and FFTs match reasonably well. A small amount of low-order harmonics appears in the simulation and experimental results, and the rms of the fundamental reaches the expected level. Inevitably, there are some very minor disagreements, caused by un-modeled phenomena and imprecise parameters such as semiconductor turn-on and turn-off times, voltage drops on the semiconductors, machine parameters, and stray capacitances.

A photograph of the experimental setup is given in Fig. 16.

VIII. CONCLUSION

This paper has presented a SVM method for the dual-inverter five-phase open-end winding topology. The algorithm is relatively easy to implement since the modulation of the multilevel converter is considered from the perspective of two five-phase two-level converters. It is shown in the paper that the dc-link voltages of the individual converters must be properly selected in order to avoid unwanted power transfer from one dc-link to the other dc-link, which may cause an unacceptable rise of the dc-link voltage of one inverter. When the modulation index is below the value of 0.57, the converter operates in two-level mode utilizing a single inverter. When the reference fundamental exceeds the capabilities of a single inverter (that is, the modulation index is more than 0.57), one inverter operates in ten-step mode, and the other is multi-frequency space vector modulated. As a result, the converter is operated in multilevel mode. The multi-frequency modulated inverter is used to add the required value to the fundamental voltage and eliminate any low-order harmonics created by the ten-step mode inverter. The method has been verified by simulation and experimental investigation.

REFERENCES

- [1] E. Levi, "Multiphase electric machines for variable-speed applications," *IEEE Trans. Ind. Electron.*, vol. 55, no. 5, pp. 1893–1909, May 2008.
- [2] P. Lezana, J. Pou, T. A. Meynard, J. Rodriguez, S. Ceballos, and F. Richardeau, "Survey on fault operation on multilevel inverters," *IEEE Trans. Ind. Electron.*, vol. 57, no. 7, pp. 2207–2218, Jul. 2010.
- [3] S. Kouro, M. Malinowski, K. Gopakumar, J. Pou, L. G. Franquelo, B. Wu, J. Rodriguez, M. A. Perez, and J. I. Leon, "Recent advances and industrial applications of multilevel converters," *IEEE Trans. Ind. Electron.*, vol. 57, no. 8, pp. 2553–2580, Aug. 2010.
- [4] P. W. Hammond, "A new approach to enhance power quality for medium voltage drives," in *Proc. IEEE Ind. Appl. Soc. 42nd Annu. Petroleum Chem. Ind. Conf.*, Denver, CO, 1995, pp. 231–235.
- [5] H. Stemmler and P. Guggenbach, "Configurations of high-power voltage source inverter drives," in *Proc. EPE Appl. Conf.*, Brighton, U.K., 1993, vol. 5, pp. 7–14.
- [6] K. A. Corzine, S. D. Sudhoff, and C. A. Whitcomb, "Performance characteristics of a cascaded two-level converter," *IEEE Trans. Energy Convers.*, vol. 14, no. 3, pp. 433–439, Sep. 1999.
- [7] B. A. Welchko and J. M. Nagashima, "A comparative evaluation of motor drive topologies for low-voltage, high-power EV/HEV propulsion systems," in *Proc. IEEE ISIE*, Rio de Janeiro, Brazil, 2003, pp. 379–384.
- [8] C. Rossi, G. Grandi, P. Corbelli, and D. Casadei, "Generation system for series hybrid powertrain based on the dual two-level inverter," presented at the EPE Appl. Conf., Barcelona, Spain, 2009, 0978.
- [9] G. Grandi, C. Rossi, A. Lega, and D. Casadei, "Multilevel operation of a dual two-level inverter with power balancing capability," in *Conf. Rec. IEEE IAS Annu. Meeting*, Tampa, FL, 2006, pp. 603–610.
- [10] L. Shuai and K. Corzine, "Multilevel multiphase propulsion drives," in *Proc. IEEE Electric Ship Technologies Symposium ESTS*, Philadelphia, PA, 2005, pp. 363–370.
- [11] Y. Kawabata, M. Nasu, T. Nomoto, E. C. Ejiogu, and T. Kawabata, "High-efficiency and low acoustic noise drive system using open-winding AC motor and two space-vector-modulated inverters," *IEEE Trans. Ind. Electron.*, vol. 49, no. 4, pp. 783–789, Aug. 2002.
- [12] G. Grandi, C. Rossi, D. Ostojic, and D. Casadei, "A new multilevel conversion structure for grid-connected PV applications," *IEEE Trans. Ind. Electron.*, vol. 56, no. 11, pp. 4416–4426, Nov. 2009.
- [13] Y. Wang, T. A. Lipo, and D. Pan, "Robust operation of double-output AC machine drive," in *Proc. IEEE ICPE ECCE Asia*, Jeju, Korea, 2011, pp. 140–144.
- [14] K. K. Mohapatra and K. Gopakumar, "A novel split phase induction motor drive without harmonic filters and with linear voltage control for the full modulation range," *Eur. Power Electron. J.*, vol. 16, no. 4, pp. 20–28, 2006.
- [15] G. Grandi, A. Tani, P. Sanjeevikumar, and D. Ostojic, "Multiphase multilevel AC motor drive based on four three-phase two-level inverters," in *Proc. Int. SPEEDAM*, Pisa, Italy, 2010, pp. 1768–1775.
- [16] E. Levi, M. Jones, and W. Satiawan, "A multiphase dual-inverter supplied drive structure for electric and hybrid electric vehicles," presented at the IEEE VPPC, Lille, France, 2010, 95-45630.
- [17] E. Levi, I. N. Satiawan, N. Bodo, and M. Jones, "A space-vector modulation scheme for multilevel open-end winding five-phase drives," *IEEE Trans. Energy Convers.*, vol. 27, no. 1, pp. 1–10, Mar. 2012.
- [18] N. Bodo, M. Jones, and E. Levi, "Multilevel space-vector PWM algorithm for seven-phase open-end winding drives," in *Proc. IEEE ISIE*, Gdansk, Poland, 2011, pp. 1881–1886.
- [19] C. M. Hutson, G. K. Venayagamoorthy, and K. A. Corzine, "Optimal SVM switching for a multilevel multiphase machine using modified discrete PSO," presented at the IEEE SIS, St. Louis, MO, 2008, 4668 326.
- [20] L. Gao and J. E. Fletcher, "A space vector switching strategy for three-level five-phase inverter drives," *IEEE Trans. Ind. Electron.*, vol. 57, no. 7, pp. 2332–2343, Jul. 2010.
- [21] O. Dordevic, M. Jones, and E. Levi, "A space-vector PWM algorithm for a three-level seven-phase voltage source inverter," presented at the EPE Appl. Conf., Birmingham, U.K., 2011, 0123.
- [22] O. López, J. Alvarez, J. Doval-Gandoy, and F. D. Freijedo, "Multilevel multiphase space vector PWM algorithm with switching state redundancy," *IEEE Trans. Ind. Electron.*, vol. 56, no. 3, pp. 792–804, Mar. 2009.
- [23] J. I. Leon, S. Vaquez, J. A. Sanchez, R. Portillo, L. G. Franquelo, J. M. Carrasco, and E. Dominguez, "Conventional space-vector modulation techniques versus the single-phase modulator for multilevel converters," *IEEE Trans. Ind. Electron.*, vol. 57, no. 7, pp. 2473–2482, Jul. 2010.
- [24] N. Bodo, E. Levi, and M. Jones, "Carrier-based modulation techniques for five-phase open-end winding drive topology," in *Proc. IEEE IECON*, Melbourne, Australia, 2011, pp. 3656–3661.
- [25] M. Jones, I. N. Satiawan, and E. Levi, "A three-level five-phase space-vector modulation algorithm based on the decomposition method," in *Proc. IEEE IEMDC*, Niagara Falls, ON, Canada, 2011, pp. 1219–1224.
- [26] A. K. Gupta and A. M. Khambadkone, "A space vector PWM scheme for multilevel inverters based on two-level space vector PWM," *IEEE Trans. Ind. Electron.*, vol. 53, no. 5, pp. 1631–1639, Oct. 2006.
- [27] G. Shiny and M. R. Baiju, "Space Vector PWM scheme without sector identification for an open-end winding induction motor based 3-level inverter," in *Proc. IEEE IECON*, Porto, Portugal, 2009, pp. 1310–1315.
- [28] D. Dujic, G. Grandi, M. Jones, and E. Levi, "A space vector PWM scheme for multifrequency output voltage generation with multiphase voltage-source inverters," *IEEE Trans. Ind. Electron.*, vol. 55, no. 5, pp. 1943–1955, May 2008.
- [29] D. Dujic, M. Jones, and E. Levi, "Continuous carrier-based vs. space vector PWM for five-phase VSI," in *Proc. IEEE EUROCON*, Warsaw, Poland, 2007, pp. 1772–1779.
- [30] A. Iqbal, E. Levi, M. Jones, and S. N. Vukosavic, "Generalised sinusoidal PWM with harmonic injection for multiphase VSIs," in *Proc. IEEE PESC*, Jeju, Korea, 2006, pp. 2871–2877.
- [31] E. Levi, D. Dujic, M. Jones, and G. Grandi, "Analytical determination of dc-bus utilization limits in multiphase VSI supplied AC drives," *IEEE Trans. Energy Convers.*, vol. 23, no. 2, pp. 433–443, Jun. 2008.
- [32] E. Levi, M. Jones, S. N. Vukosavic, and H. A. Toliyat, "A novel concept of a multiphase, multi-motor vector controlled drive system supplied from a single voltage source inverter," *IEEE Trans. Power Electron.*, vol. 19, no. 2, pp. 320–335, Mar. 2004.
- [33] M. Jones, D. Dujic, E. Levi, and S. N. Vukosavic, "Dead-time effects in voltage source inverter fed multiphase AC motor drives and their compensation," presented at the EPE Appl. Conf., Barcelona, Spain, 2009, 0001.
- [34] M. Jones, S. N. Vukosavic, D. Dujic, and E. Levi, "A synchronous current control scheme for multiphase induction motor drives," *IEEE Trans. Energy Convers.*, vol. 24, no. 4, pp. 860–868, Dec. 2009.



Martin Jones received the B.Eng. degree (First Class Honors) in electrical engineering from Liverpool John Moores University, Liverpool, U.K., in 2001. He was a research student at Liverpool John Moores University from September 2001 until Spring 2005, when he received the Ph.D. degree. Mr Jones was a recipient of the IEE Robinson Research Scholarship for his Ph.D. studies.

He is currently a Reader at Liverpool John Moores University. His research is in the area of high-performance ac drives.



I. Nyoman Wahyu Satiawan was born in Singaraja, Bali, Indonesia, in 1970. He received the first degree in electrical engineering from the University of Udayana, Bali, Indonesia, in 1996, and the M.Sc. degree in control engineering and the Ph.D. degree from Liverpool John Moores University, Liverpool, U.K., in 2001 and 2012, respectively.

He joined the University of Mataram, West Nusa Tenggara, Indonesia, as an academic in 1998. His research interests are in the area of electric motor drives and power converters.



Nandor Bodo (S'11) received the Master's degree in power electronics from the University of Novi Sad, Novi Sad, Serbia, in 2009. Currently, he is working toward the Ph.D. degree at Liverpool John Moores University, Liverpool, U.K.

His research interests include power electronics and variable-speed drives.



Emil Levi (S'89–M'92–SM'99–F'09) received the M.Sc. and Ph.D. degrees from the University of Belgrade, Belgrade, Yugoslavia, in 1986 and 1990, respectively.

From 1982 until 1992, he was with the Department of Electrical Engineering, University of Novi Sad. He joined Liverpool John Moores University, Liverpool, U.K., in May 1992 and has been, since September 2000, a Professor of Electric Machines and Drives.

Prof. Levi serves as an Editor of the IEEE TRANSACTIONS ON ENERGY CONVERSION, a Co-Editor-in-Chief of the IEEE TRANSACTIONS ON INDUSTRIAL ELECTRONICS, and as the Editor-in-Chief of the *IET Electric Power Applications*. He was the recipient of the Cyril Veinott Award of the IEEE Power and Energy Society for 2009 and the Best Paper Award of the IEEE TRANSACTIONS ON INDUSTRIAL ELECTRONICS for 2008.